#1243

J. theor. Biol. (1993) **160,** 471–491

Somatic Mutation, Monoclonality and Stochastic Models of Stem Cell Organization in the Intestinal Crypt

MARKUS LOEFFLER†‖, ANDREAS BIRKE†, DOUGLAS WINTON‡ AND CHRISTOPHER POTTEN§

† *Department of Biometry, Klinik I für Innere Medizin der Universität zu Koeln, LFI-Ebene* 5, *Joseph-Stelzmann-Strasse* 9, *D*-5000 *Köln* 41, *Germany,* ‡ *CRC Department of Pathology, University of Cambridge, Tennis Court Road, Cambridge CB*2 1*QP and* § *CRC Epithelial Biology, Paterson Institute, Christie Hospital (NHS) Trust, Wilmslow Road, Manchester M*20 9*BX, U.K.*

(*Received on* 1 *February* 1992, *Accepted in revised form on* 2 *August* 1992)

Among highly proliferating tissues the intestinal tissue is of particular interest. Techniques are available that permit an insight into how intestinal crypts as the basic macroscopic tissue unit are regenerated from a small population of self-maintaining stem cells. However, neither the precise number of these stem cells nor their properties are known.

We have recently suggested a model of stem cell organization which explains the life cycle of murine intestinal crypts, their birth (by crypt fission) and extinction rates, as well as their size distribution on a quantitative basis (Loeffler & Grossman, 1991). The model assumptions involve two stochastic branching processes, one for the growth of several independent indistinguishable stem cells and a second for a threshold dependent crypt fission process.

New data have now become available challenging the above concept. They relate to the conversion of crypts to monoclonal phenotypic expression after mutagenic events, presumably taking place in single stem cells. A detailed analysis of these data is shown here utilizing a more elaborate version of the above model. The new data are consistent with this model within the range of parameters predicted previously.

We conclude that the cellular regeneration of intestinal crypts can be explained on the basis of several indistinguishable stem cells which can replace each other.

Introduction

It has become clear in the last few years that an understanding of epithelial tissues requires a profound insight into the organization and control of the epithelial stem cells. Stem cells represent a very small minority of cells able to maintain and repopulate the entire tissue and are therefore ultimately responsible for the functional integrity of the organ. Despite most intensive examination, the precise nature of stem cell organization in the intestinal epithelium has resisted elucidation (see review by Potten & Loeffler, 1990).

‖ Author to whom correspondence should be addressed.

0022-5193/93/040471+21 $08.00/0

© 1993 Academic Press Limited

The murine small intestinal epithelium has attracted attention for several reasons: First, the regenerating units are clearly defined. All proliferation takes place in small bag-shaped anatomical structures, called the crypts, containing about 250 cells of which 150 are proliferating. Second, although the proliferating cells in the crypts divide very rapidly and about 300 cells leave each crypt per day, the macroscopic appearance of the crypt is stable. Third, there is good evidence based on regeneration bioassays that not all proliferating cells can guarantee crypt survival but only a small subpopulation. However, so far no techniques are available to reliably identify and count these cells.

With respect to the precise organization of the crypt stem cells various views exist. They primarily differ in one respect: Are they all indistinguishable (equivalent) or do they differ from one another (for example, age structured)?

Two such views have been proposed recently by us and other authors. They can briefly be summarized as follows:

CONCEPT OF A STEM CELL PEDIGREE

Winton & Ponder (1990) presented interesting data on an intestinal mutation assay (see below). They interpret the data as showing that there is a single infrequently dividing *master stem cell* that maintains the epithelium of each crypt through a population of *descending transit or temporary stem cells* which are cycling more frequently. Some of the transit stem cells are rapidly dividing and exactly self-maintaining for as long as 12 weeks. This implies that the active stem cells in the crypt are arranged as a stem cell predigree originating from a slowly cycling single stem cell at its apex. Similar views are shared by Meinzer *et al.* (1992). These authors included a programmed senescence of stem cells with the entire crypt ultimately depending on one single master stem cell. For simplicity we call this the stem cell pedigree concept.

CONCEPT OF FUNCTIONALLY EQUIVALENT STEM CELLS

In contrast to this hypothesis, Potten & Loeffler and collaborators (1986, 1987, 1991) proposed the *concept of functionally equivalent stem cells*. They suggested that in the normal steady state a number of indistinguishable stem cells coexist in each crypt. All of them have the same potential to repopulate the crypt and all grow according to the same growth process, i.e. with the same average cell cycle times and self-maintaining probabilities. This concept was modelled mathematically and was shown to be in agreement with a broad spectrum of data on the short-term (days) behaviour of cell replacement in a crypt and on long-term behaviour (months) of populations of crypts (Loeffler & Grossman, 1991).

It is the objective of this communication to show that the data presented by Winton & Ponder (1990) on the development of monoclonal crypts are also consistent with the concept of functionally equivalent stem cells and that the process of conversion of monoclonal crypts provides further insight into stem cell organization.

Data on Mutations and Crypt Conversion to a New Monoclonal Phenotypic Expression

Winton & coworkers (1988, 1990) studied the spread of cellular clones induced by somatic mutation in the jejunal crypt. They used heterozygous *Dlb-1b/Dlb-1a* mice whose intestinal epithelial cells stain positively with a peroxidase conjugate of *Dolichos biflorus* agglutinin (DBA-Px). Mutation of the Dlb-1b locus in stem cells results in the loss of DBA-Px binding and this becomes recognizable as wholly or partly unstained (negative) crypts. Mutations occur spontaneously at a low rate and can be induced by treatment with cytotoxic alkylating drugs such as ethylnitrosurea (ENU).

The most important findings of Winton & Ponder (1990) can be summarized as follows (see Fig. 1):

(1) After ENU-treatment a small number of crypts develop which exclusively contain negative cells. These crypts have converted from a positively staining P-monoclonal to a new negatively stained N-monoclonal state (short: from P-monoclonality to N-monoclonality, from P-state to N-state). The first N-crypts are already

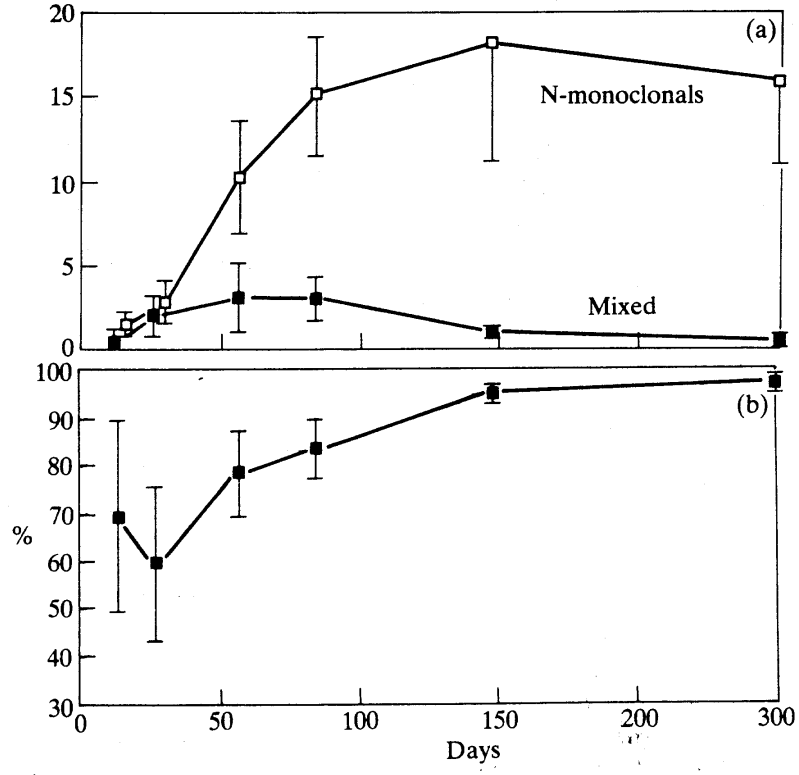

FIG. 1. Experimental data on the time course of the incidence of mutated crypts following ENU treatment of mice. (a) Absolute incidence of fully mutated negatively stained crypts (□) and of crypts containing mixtures of positive and negative cells (■) per 10 000 crypts scored. Means and standard deviations are given. (b) Ratio of N-monoclonal crypts and all crypts containing mutated cells (monoclonal and detectable mixed), redrawn and recalculated from Winton & Ponder (1990). As can be seen after 2 weeks, about 60% of the crypts containing N-cells are monoclonal and 90% after 100 days.

found 2 weeks after ENU treatment. Their number continues to increase and reaches a maximum after about 150 days.

(2) After ENU-treatment a number of crypts develop which contain a mixture of positively and negatively stained cells (called mixed crypts, M-crypts for short). Initially N-crypts and mixed crypts are equally frequent [Fig. 1(a)]. Later, the absolute number of mixed crypts exhibits a temporary increase, peaking between day 50 and 80. The peak frequency is about one-fifth of the negative crypts. In the long run mixed crypts become rare [Fig. 1(a)]. Figure 1(b) displays the data in a different way, showing which percentage of all crypts identified as containing mutated cells is indeed N-monoclonal.

(3) Owing to the microscopic technique (stained Paneth cells may project onto and therefore obscure negatively stained mid and upper crypt cells) it may often be difficult to identify a crypt with a few negative cells as a mixed crypt. It will often be erroneously classified as a P-crypt unaffected by somatic mutation. Consequently there is a detection threshold for identifying a true mixed crypt as such. It is, however, not clear how big this detection threshold is and how many true mixed crypts are overlooked.

(4) Throughout days 15–200 different types of mixed crypts (with, for example, 25%, 50%, 75% negative cells) exist in almost constant fractions (Winton, unpublished observations).

Basic Assumption of the Concept of Functionally Equivalent Stem Cells

We briefly summarize the essential assumptions of the corresponding model (see Fig. 2) (Potten & Loeffler, 1990; Loeffler & Grossmann, 1991):

ASSUMPTION 1 (STEM CELLS)

A number of actual stem cells (S) exist, each of which is equally able to populate the entire intestinal crypt and maintain it (see also the definition for actual stem cells in Potten & Loeffler, 1990).

ASSUMPTION 2 (STOCHASTIC CELL DIVISION)

In the steady state each of these cells behaves independent of the others and independent of its own history. The growth process can be described by a stochastic branching process where a stem cell produces either 2, 1 or zero stem cell offsprings with probabilities p, r and q ($p+r+q=1$) [see Fig. 2(a)].

ASSUMPTION 3 (THRESHOLD-DEPENDENT CRYPT FISSION)

Crypts divide if the number of stem cells (S) exceeds a certain threshold number, S_f. In this case the stems cells are distributed to the daughter crypts according to binomial statistics. A crypt with zero stem cells is considered extinct [see Fig. 2(b)].

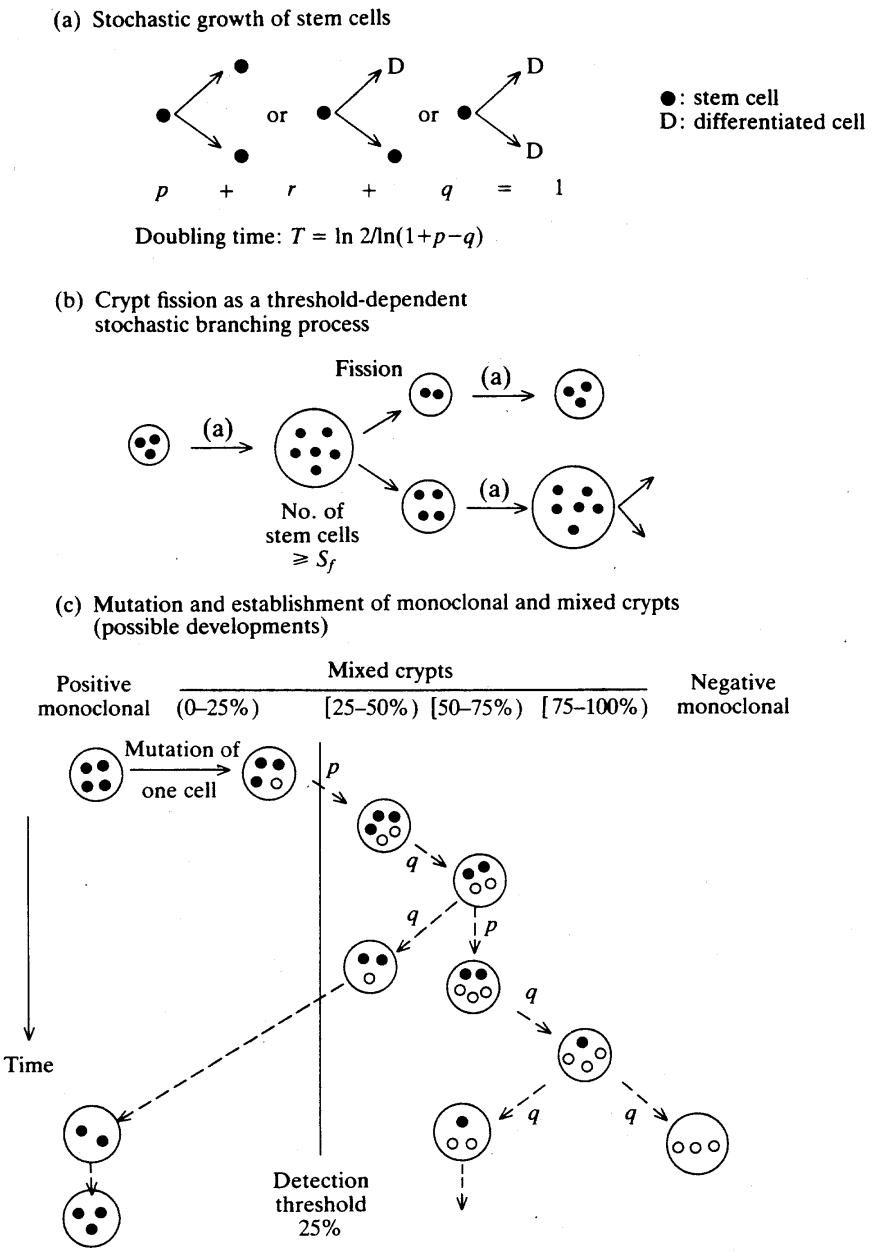

FIG. 2. Model scheme. Three processes are displayed. (a) Cellular growth process of the stem cells: A stem cell can produce either 2, 1 or zero stem cells with probabilities p, r, and q. (b) Crypt fission process: If the number of stem cells exceeds a certain threshold value the crypt divides and the cells are distributed according to binomial statistics (full arrows). (c) Possible development of mutations in a single crypt. All stem cells grow alike. The mutated cells can either disappear owing to differentiation or generate one or two mutated stem cells. Thus the mixture can change as displayed in this example and the crypt can turn to monoclonality of either type (positive or negative). Possible developments are shown by dashed arrows. Mixed crypts can be categorized in classes according to the percentage of N-cells included [M_{I}: (0–25%), M_{II}: [25–50%), M_{III}: [50–75%), M_{IV}: [75–100%)].

The number of crypts is assumed to grow with a doubling time T. This implies a constraint on p, r and q since $(2p+r)^T=2$.

ASSUMPTION 4 (PROPORTIONALITY OF CRYPT SIZE AND NUMBER OF STEM CELLS)

In the steady state there is a population of differentiating cell stages (D-cells), which undergo a fixed number of cell divisions (amplification). Consequently the size of a crypt is proportional to the number of stem cells present.

ASSUMPTION 5 (EFFECT OF Dlb-1b MUTATIONS)

Initial condition: Each stem cell has the same probability of experiencing a Dlb-1b mutation irrespective of the crypt in which it is located. Mutations are rare so that two or more mutations per crypt can be neglected;

Effect on growth: The mutations are neutral with respect to the stem cell growth process, i.e. no effect on the values of p, r, q has to be assumed. Mutations are fixed and transferred to all daughter cells and offspring stem cells originating from the mutated stem cells.

ASSUMPTION 6 (DETECTION THRESHOLD)

There is a detection threshold (d) for identifying mutations in crypts. Mixed crypts with a fraction of mutated cells less than d will be scored as unaffected.

Assumptions 1–4 are identical to those presented in Loeffler & Grossmann (1991). Parameters consistent with the data on growth of crypt population were identified as $S_f \geq 8$ and $r \geq 0{\cdot}8$.

According to the growth process described in the above model, mixed crypts will change with time. The number of stem cells, as well as the mixture, can change. Mixed crypts are not stable in the long run and they will end in one of the absorbing states as either N-monoclonal or P-monoclonal crypts. There can be a variety of mixed crypts with different degrees of mixture. Mixed crypts with few negative cells may erroneously be counted as P-monoclonal in experiments. The extent of this underscoring of mixed crypts depends on the detection threshold (d).

The technical details of this concept, the algorithm used and the evaluation procedures adopted in model simulations are straightforward and can be found in the Appendix.

Results

STATIONARY DISTRIBUTION OF STEM CELLS PER CRYPT

In order to investigate how rapidly mutations of single stem cells can spread and affect an entire crypt, it is important to consider that crypts might differ in the number of stem cells. The present model accounts for this problem by generating a

stem cell distribution per crypt as a result of the stochastic stem cell growth and crypt fission process. Stationary steady-state distributions of stem cells per crypt can be obtained either by direct simulation using Monte Carlo techniques, or through iterative renormalization procedures as shown by Loeffler & Grossman (1991). Figure 3 shows a comparison of both for an example assuming a fission threshold of 16 and a probability of asymmetric division of 0·99. While the open symbols describe the results of the Monte Carlo simulation based on single cell descriptions, the closed symbols describe the results of the direct approximation of the iterative renormalization procedure of the entire distribution. The comparison shows good agreement for this example. In general, consistency was found between both approaches. Consequently, the Monte Carlo simulation could be used to describe the behaviour of single cells in crypts without losing consistency with previous model results on the distributions.

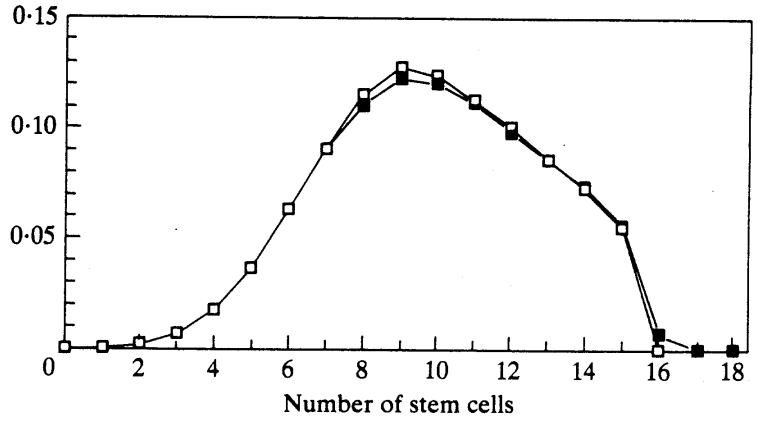

FIG. 3. Stationary stem cell distributions per crypt. An example is given to compare the stationary stem cell distribution of the Monte Carlo calculations (□) and those calculated by a more exact procedure in Loeffler & Grossmann (1991) (■). The parameters used are: $S_f = 16$, $r = 0{\cdot}99$, $T = 100$.

MUTATION

As each stem cell is assumed to mutate with the same probability, crypts with many stem cells are likely to be more frequently affected by a mutation. As the mutation frequency is in fact small in the experiments, one can reasonably assume that the probability for a crypt to contain one mutated stem cell is proportional to the number of stem cells present. Consequently the distribution of stem cells in those crypts containing a mutated stem cell will be different from the stationary distribution discussed above (i.e. skewed to the right). Thus, to simulate this feature of the mutation process an appropriately stratified random sample of crypts was selected from a stationary population of crypts containing a single mutated cell.

CONVERSION TO MONOCLONALITY WITH TIME

Conversion of crypts initially containing mutated stem cells occurs with time and depends on the specific parameters chosen. To illustrate the principal features Fig. 4 exhibits a series of model simulations for one specific set of parameters ($S_f=8$, $r=0{\cdot}93$, $T=400$). Figure 4(a) shows how the percentage of N-monoclonal, P-monoclonal and mixed crypts changes with time. Initially only a few N-monoclonal crypts and many mixed crypts are present. After a while, many of the mutated stem cells are lost and most of the crypts return to the unmutated P-monoclonal state. In the long run, in this example, 81% of the crypts which started off with a mutation lost it by differentiation of the stem cell [shaded area in Fig. 4(a), see also Fig. 2(c)]. However, there is also a fraction of mixed crypts in which the number of N-cells increases while the P-cells disappear. This process generates fully negative N-monoclonal crypts [Fig. 2(c)]. In the long run, all mixed crypts convert to either P or N-monoclonality.

Experimentally data corresponding to Fig. 4(a) are not available because the number of initially mutated cells cannot be assessed at present. Consequently the number of mixed crypts returning to P-monoclonality is not measurable experimentally. For practical reasons one has to restrict the experimental evaluations to those crypts which actually contain a detectable number of mutated cells. It is, however, important to understand that mixed crypts with only a few mutated cells will be overlooked in the experimental scoring procedure. Therefore the effect of a detection threshold has to be considered in the following model simulations.

Figure 4(b) shows how the ratio of N-monoclonal crypts to all crypts containing detectable numbers of mutated cells develops with time. Three curves are given applying three different detection thresholds to the same simulation ($d=0{\cdot}3$, $0{\cdot}50$, $0{\cdot}60$ from bottom to top, respectively). As the curves in Fig. 4(b) show, the detection threshold has a remarkable effect on the shape and level of the curves in the initial phase. In general, lower detection thresholds imply deeper nadirs of the curves.

The simulations in Fig. 4(b) can directly be compared with the data in Fig. 1(b). The earliest measurements were performed 14 days after injection of the mutagen showing that 83% of the crypts are N-monoclonal at this time and 59% at day 28. If one assumes that a cell cycle time in the model (one generation) corresponds to 1 day ($t_c=1$ day, which is realistic for small intestine stem cell (Potten & Loeffler 1990), the model simulations fit the data in Fig. 1(b) provided the detection threshold is somewhat less than $d=0{\cdot}5$ (middle case).

Clearly a systematic search was required to find the set of model parameters (S_f, r, t_c, d) consistent with the published data. A systematic variation of these parameters was therefore performed and a series of curves like those in Fig. 4(b) were evaluated. The results for a cell cycle time of 1 day are summarized in Table 1 (rows labelled A). A comparison of the values in Table 1 with the data in Fig. 1 shows that a restricted subset of model scenario is indeed consistent with the data.

Figure 4(c) shows another way of comparing model simulations with experimental data. It displays the time course of the concentration of N-monoclonal crypts and detectable mixed crypts among the entire population of crypts. The concentration of

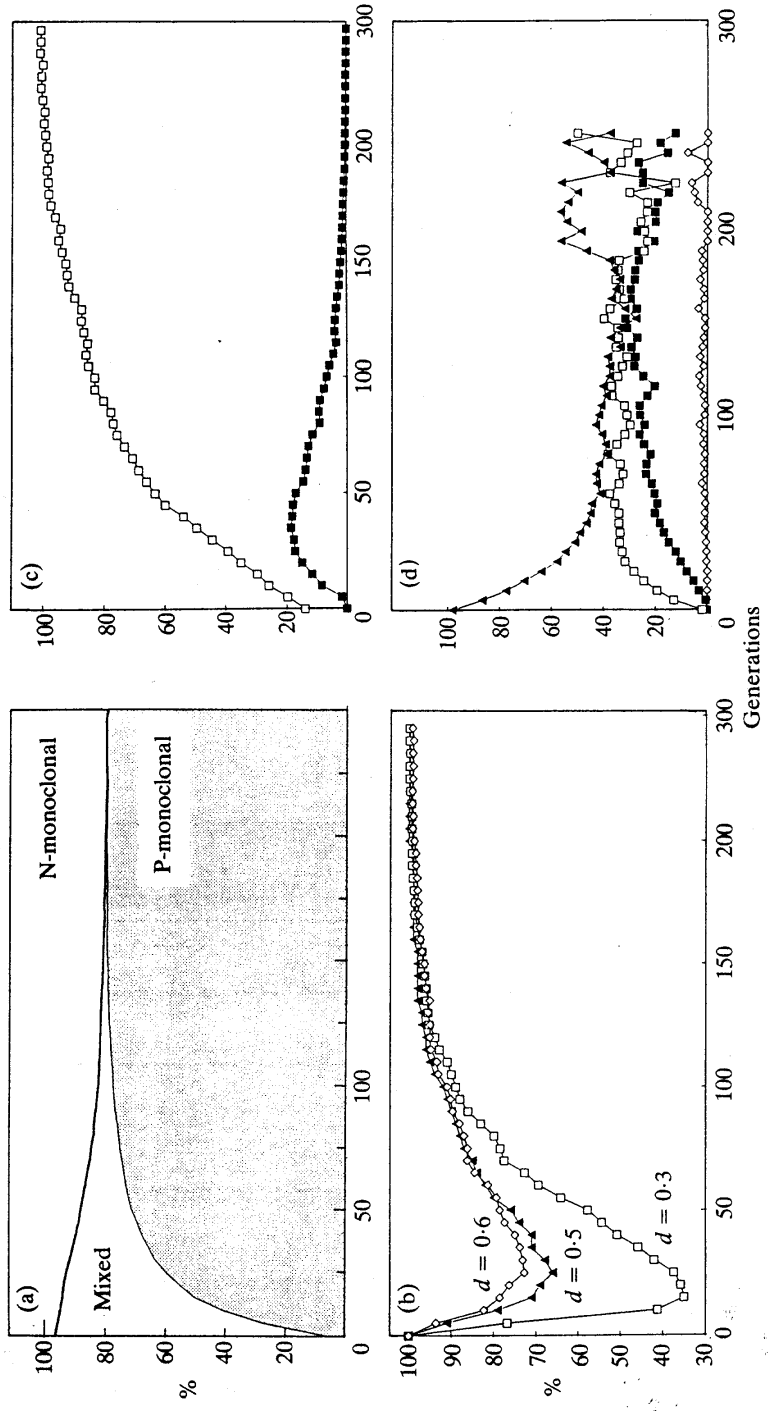

FIG. 4. Conversion of crypts to monoclonality. Examples for model simulations with one set of parameters ($T = 400$, $r = 0{\cdot}93$, $S_f = 8$). In each model crypt exactly one stem cell was mutated initially. (a) N-monoclonal, P-monoclonal and mixed crypts with time. It is apparent that most of the initial mutations disappear rapidly and normal P-monoclonal crypts remains while a minority are converted to N-monoclonality. (b) The fraction of N-monoclonal crypts containing a detectable number of M-cells. Three different curves are shown in which different detection thresholds hold ($d = 0{\cdot}30$, $0{\cdot}50$, $0{\cdot}60$). The diagram is comparable with Fig. 1(b). (c) Time course of the concentration of N-monoclonal crypts and of mixed crypts with a detection threshold of 0·40. The picture can be compared with Fig. 1(a). (■), Detectable mixed; (□), N-monoclonals. (d) Time course of different classes of mixed crypts M_{I} (▲), M_{II} (□), M_{III} (■) and M_{IV} (◇).

TABLE 1(a)

Summary of Monte Carlo simulations ($t_c = 1$ *day*) *detection threshold*, d = 0·0

S_f	r		Time course (days) 0	15	30	60	Fraction of crypts converted
4	0·970	A:	28	36	51	73	0·50
		B:	141	90	58	27	
6	0·953	A:	12	21	39	69	0·32
		B:	262	136	79	31	
8	0·900	A:	7	15	32	67	0·25
		B:	342	159	90	31	
10	0·865	A:	5	12	28	65	0·18
		B:	472	193	109	38	

The model scenarios are selected in such a way that all exhibit a 90% conversion to monoclonality in 100 generations. For any detection threshold d only specific sets of values S_f and r fulfil this criterion. They are given in the left two columns of each sub-table. Two rows are given for each constellation. The first row (A) gives the percentage of N-monoclonal crypts detectable on days 0, 15, 30, and 60, respectively $[N(t)/N(t)+M_d(t)]$ and the fraction of crypts initially containing an N-Cell finally converted to N-monoclonality $[N_\infty = \lim_{t\to\infty} N(t)/A(t)]$ [comparable to Fig. 1(b)]. The second row (B) describes the time course of the detectable mixed crypts expressed as percentage of the final plateau concentration of N-monoclonal crypts $[100 \times M_d(t)/N\infty]$ [comparable to Fig. 1(a)]. The boxed scenario are consistent with the experimental data in Fig. 1(a) and (b).

TABLE 1(b)

Detection threshold, d = 0·30

S_f	r		Time course (days) 0	15	30	60	Fraction of crypts converted
4	0·987	A:	98	88	84	86	0·45
		B:	1	10	12	12	
6	0·955	A:	88	57	58	76	0·35
		B:	3	26	27	17	
8	0·920	A:	79	44	48	72	0·26
		B:	6	52	56	27	
10	0·890	A:	77	35	42	69	0·21
		B:	5	59	58	32	

mixed crypts shows a peaking characteristic. The peak values differ considerably depending on the detection thresholds. These curves can be compared to the data in Fig. 1(a), where the number of crypts containing mutations is given per 10^5 crypts scored.

In the data, the maximum peak concentration of mixed crypts reaches 20–30% of the final plateau concentration of N-monoclonal crypts. This ratio has also been evaluated for different model scenario and results are also given in Table 1 (rows labelled B). The scenario which are consistent with the experimental data are boxed

TABLE 1(c)

Detection threshold, d = 0·40

S_f	r		Time course (days) 0	15	30	60	Fraction of crypts converted
4	0·987	A:	98	89	85	87	0·43
		B:	6	80	78	37	
6	0·957	A:	97	73	66	76	0·30
		B:	2	19	26	20	
8	0·927	A:	93	57	55	73	0·24
		B:	2	27	30	20	
10	0·892	A:	86	42	49	74	0·15
		B:	2	39	40	23	

TABLE 1(d)

Detection threshold, d = 0·50

S_f	r		Time course (days) 0	15	30	60	Fraction of crypts converted
6	0·96	A:	97	92	88	92	0·34
		B:	0	4	7	7	
8	0·93	A:	93	81	77	87	0·26
		B:	0	10	15	12	
10	0·905	A:	91	72	68	80	0·19
		B:	0	12	19	17	
12	0·87	A:	80	63	62	80	0·17
		B:	0	16	25	17	
14	0·85	A:	87	60	57	78	0·15
		B:	0	19	27	18	
16	0·82	A:	82	56	56	74	0·12
		B:	0	23	33	24	

in Table 1. They fit the experimental data displayed in Fig. 1(a) and (b) with the peak height of mixed crypts in the order of 30% of the N-monoclonal plateau and with a 50–70% trough in the ratio. A necessary requirement for a good model fit is apparently $d \geq 0{\cdot}30$ and $S_f \geq 6$.

Figure 4(d) describes another model feature which can directly be compared to the experimental data. The evaluation is restricted to mixed crypts. They are categorized into four classes according to the percentage of N-cells present (i.e. class M_I: below 25%, class M_{II}: 25–50%, class M_{III}: 50–75%, class M_{IV}: above 75%). As the crypts start with one mutated cell, class M_I is most frequent initially. With time, however, the N-cells become more frequent and the other classes of mixed crypts fill up consecutively. After about 50 generations in this example a steady state is reached in which all classes exhibit constant percentages. As the mutation is neutral with

respect to stem cell growth, mutated stem cells have the same chance of growing as non-mutated cells. Consequently there are, on average, as many losses and gains of mutated and non-mutated cells. This explains that the number of crypts switching, for example, from class M_{III} to class M_{II}, balances the number of crypts going from M_{II} to M_{III}. In other terms, there is a steady state of dynamic class changes in this phase. This plateau phase is terminated by a phase of strong fluctuations which are due to the final loss of all mixed crypts. Experimental observations about the time behaviour of the different size classes of mixed crypts are limited, but available data indeed show constant ratios with the majority of mixed crypts having between 25–75% of N-cells (Winton, unpublished data).

Selection of Model Parameters

In the previous paragraph, examples for time courses were discussed. It was demonstrated that a fit of the model to the experimental data is possible for specific combinations of the model parameters. In fact, one can delineate the set of parameters further, for which the model is consistent with the data.

CRYPT DOUBLING TIME T

One may question whether crypt fission is a relevant mechanism to generate N-monoclonal crypts from mixed mother crypts. For any given set of parameters $S_f \geq 6$ and $r \geq 0{\cdot}8$ we found that only a few percent of the conversions to N-monoclonality are a result of the fission process. Varying the crypt doubling time between 50 and 10 000 cell cycles hardly affected the time to monoclonal conversion. This is understandable as it is rare in the model that a mixed crypt divides in such a way that one or even two monoclonal crypts result. Thus in these circumstances cell division is a much more important contributor to conversion to crypt monotonically than crypt fission. For all practical purposes the calculations can therefore be undertaken with $T=400$ and the five dimensional parameter space effectively reduces to four dimensions.

CELL CYCLE TIME t_c

The cell cycle time t_c is relevant in selecting model parameters consistent with the data. Fig. 5(a) displays those combinations of S_f and r which yield a 90%-conversion in 100 days given the detection threshold $d=0$. The dots represent models where one generation corresponds to 1 day ($t_c=1$). The set of models is denoted by a relationship of S_f and r which is remarkably linear. The two other curves represent models with a cell cycle time of 2 days ($t_c=2$) or 0·5 days ($t_c=0{\cdot}5$). The slope of the curves depends on the choice of t_c. A shorter cell cycle time requires a higher r to be consistent with a 90% conversion in 100 days. Less frequent cell divisions are consistent with less stringent conditions for r.

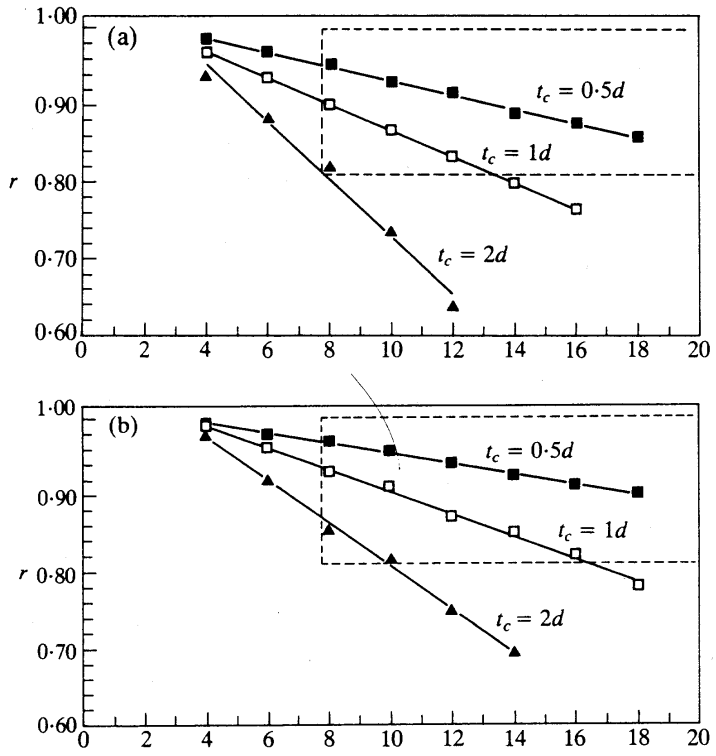

FIG. 5. Parameter space consistent with experimental data. Each point (square, triangle) in the S_f-r diagram represents one model which generates a 90% conversion to monoclonality within 100 days (isoconversion models). (a) Isoconversion models for a detection threshold of $d=0$. The three curves differ with respect to the cell cycle time (t_c: 0·5, 1, 2 days). The boxed area indicates which set of parameters was found compatible with a previous model on crypt fission, extinction and crypt size distribution (Loeffler & Grossmann, 1991). (b) Isoconversion models for a detection threshold of $d=0{\cdot}50$ [otherwise like (a)].

DETECTION THRESHOLD d

The detection threshold d is also relevant for selecting reasonable models. Figure 5(b) gives the iso-set of model parameters consistent with a 90%-conversion to monoclonality within 100 days, assuming a detection threshold of $d=0{\cdot}5$ and cell cycle times t_c of 0·5, 1 and 2 days. Comparing Fig. 5(a) and (b) it is evident that all curves shift upwards towards higher r with increasing value of d. For cell cycle times of 0·5 and 2 days, simulations have been systematically generated similar to those in Fig. 4(b) and (c) and Table 1. The model scenario consistent with the experimental data shown in Fig. 1 is summarized in Table 2.

Consistency with the Previous Model

Originally our model was invented to describe observations on crypt growth including crypt fission frequency, crypt extinction, and size distributions. Based on a cell

TABLE 2

Parameters of model scenario consistent with the data

Cell cycle time t_c	Fission threshold S_f	Division probability r	Detection threshold d
0·5 days	6	0·977	0·3
	8	0·965	0·4
	10	0·955	0·5
	12	0·935	0·5
	14	0·925	0·5
	16	0·910	0·5
1 day	6	0·955	0·3
	6	0·957	0·4
	8	0·927	0·5
	10	0·905	0·5
	12	0·870	0·5
	14	0·850	0·5
2 days	8	0·855	0·4
	10	0·820	0·5

cycle time of 1 day it was concluded (Loeffler & Grossman, 1991) that the crypt fission threshold S_f should be 8 or more and that r should be 0·8 at minimum. As displayed in Fig. 5(a) and (b) there is a considerable range of parameters left for which full consistency with data both on crypt growth and conversion to monoclonality can be found. Thus the new set of data on conversion of monoclonality is in agreement with the previous model conclusions.

Estimates of Cell Mutation Frequencies

In the model the majority of crypts containing mutated cells in the beginning do not develop into N-monoclonal crypts. Generally speaking only one out of five stem cell mutations succeeds in establishing a N-monoclonal crypt. Table 1 gives more detailed numbers (last column).

Life Time of Crypts

The present model allows the calculation of a distribution of life times for individual crypts. For $r=0·6$ and 0·9 the average life time of individual crypts is in the order of less than 100 generations, although the doubling time of the total crypt number is 400 generations. This is a result of rather frequent loss of crypts by extinction. For $r>0·95$ the average life times are in the order of the doubling time of the crypt number and the distribution exhibits a large coefficient of variation. No data on lifetime distributions of crypts are presently available to compare with these model results, but once available may help to establish further constraints on the selection of adequate model parameters.

Spontaneous Mutation

One new N-monoclonal crypt is formed per week spontaneously per 10^6 crypts. At any time one finds two detectable mixed crypts per 10^6 crypts, indicating that the life span of such mixed crypts averages at about 2 weeks. This is consistent with the transitory nature of mixed crypts after mutagenic induction.

Discussion

The model presented here allows a comprehensive quantitative understanding of intestinal crypt growth and regeneration over long time scales (up to several 100 days). The basic model assumption is that a number of functionally equivalent and indistinguishable actual stem cells exist which can produce two, one (most frequently) or no daughter stem cells. The decision between these options is stochastic. Crypts with too many stem cells divide and segregate their stem cells to daughter crypts according to a binomial process. The model requires specification of four relevant parameters: the crypt fission threshold (S_f), the probability of asymmetric stem cell division (r), the detection threshold (d) and the cell cycle time t_c. Consistency with data on crypt birth, extinction and conversion to monoclonality can be obtained if the following restrictions for the parameters hold: $d \geq 0{\cdot}4$ (detection threshold); $S_f \geq 8$ (fission threshold); $r \geq 0{\cdot}8$ (probability of asymmetry division); $0{\cdot}5 \leq t_c \leq 2$ (cell cycle time in days).

The above analysis shows that the concept of coexisting functionally equivalent stem cells in a crypt cannot be dismissed on the basis of the data presently available. The present concept is also consistent with previous models describing the crypt regeneration over short time scales (days) where symmetric stem cell divisions can be neglected (see Loeffler *et al.*, 1986, 1987, 1988).

Furthermore, the present model has a number of implications which should be examined by further experiments. First, the analysis indicates that the experimental procedure used by Winton & Ponder (1990) did not detect a considerable number of mixed crypts (the threshold problem). This was a result of their scoring procedure at low magnification from the exterior side of a gut. Thus, positively stained Paneth cells located of the crypt base may have covered unstained negative columnar cells which projected behind them. The magnitude of this detection problem should be investigated in more detail.

Second, the stem cell cycle time has a marked effect on the time to conversion. Animals with faster cell cycle times should achieve the conversion to monoclonality earlier. Likewise, long-lasting manipulations of the cell cycle time should affect the conversion time.

Third, the model predicts that the cellular mutation rate is several fold higher than the final number of N-monoclonal crypts would indicate. Consequently the mutagenicity of ENU on stem cells might be considerably underestimated if only based on numbers of N-monoclonal crypts observed.

Fourth, a way to challenge the model is to gather more detailed measurements on the distribution of lifetimes of individual crypts. Measurements should be conducted

on cohorts of ENU-treated animals to examine how many N-monoclonal crypts are present as single crypts, pairs or triplets of adjacent N-crypts surrounded by positive crypts. With time the single N-monoclonal crypts should divide to form two or three crypts which stay adjacent to each other. From the transition of single N-crypts to pairs the lifetime could be deduced. This would then allow a more precise lower estimate of r to be used, and by virtue of Fig. 5 it would narrow the options of S_f.

Fifth, this model predicts stochastic fluctuations in the ratio of normal P-cells and N-cells in individual crypts. In any given single crypt the mixture of P-cells and N-cells can change in an unpredictable way. The percentage of N-cells can increase and decrease repeatedly until the crypt finally ends in one of the absorbing monoclonal states. Unfortunately, at present, it is not possible to pursue these fluctuations in single crypts. However, it may be possible to investigate this prediction experimentally by examining carefully the shape of the ribbons of negatively stained cells which stretch from the bottom of the villus to its tip. The model predicts that there should be jumps in the width of these ribbons.

Assuming the acceptable parameter sets given in Table 1 and considering the fact that the cells need at least 1 day to move across a villus, one can estimate the frequency of changes of ribbon width to be expected in the experiments. Under these circumstances it is also reasonable to assume that most continuous uninterrupted ribbons require at least $1/3\ S_f$ mutated stem cells in a crypt in order to be visible. The probability that all of these stem cells are lost by differentiation in a 1 day interval (the transit time through the middle of the villus) is less than 1 out of 1000. Thus a complete cessation of well established continuous ribbons should be seen but only at a low frequency. Likewise jumps in ribbon width should be detectable. Their frequency would depend on the magnitude of the jump in width (i.e. the greater, the rarer) and the values of p, q, and r. The range of frequencies predicted by the various model scenarios is fairly broad. Depending on the choice of parameters one can expect jumps in ribbon width of ±25–50% to occur in a frequency between 1 out of 10 000 and 1 out of 100. Thus experimental observation of these quantities should allow to discern the model scenario in more detail. The best time to investigate these conditions should be between day 10 and 50 after ENU.

This prediction of stochastic fluctuations in ribbon width is at odds with the implications of the concept of a stem cell pedigree maintained by a master stem cell. In the latter concept mixed crypts would contain a constant mixture of P- and N-cells for a certain time and then lose all N-cells. Thus this latter concept does not predict fluctuations in the widths of villus ribbons, but rather a succession of different ribbons originating from different crypts. Narrow ribbons originating from crypts with a small number of N stem-cells would appear first. When these crypts convert back to P-state other crypts form new and broader ribbons. Thus a succession of mixed crypts should be expected if this concept holds until finally only N-monoclonal crypts appear. All mixed crypts will end in the P-monoclonal state. Only a mutation of the master stem cell can establish a permanent N-monoclonal crypt. These considerations illustrate that more experimental details on the fluctuation and the succession of mixed states and changes in ribbon widths might allow one to distinguish between the two concepts.

The model and data discussed so far relate to the small intestinal murine crypts. It will be challenging to see whether the concept more generally applies to the same tissue in other animals and humans or to other parts of the gut. Recently, experiments were reported by Griffith *et al.* (1988) investigating somatic mutation and conversion to monoclonality in the murine colonic crypt using as a marker an expression pattern of X-linked G6PD enzyme activity. They observed that after an 8 week treatment with alkylating drugs there were negatively stained monoclonal colonic crypts but almost no mixed crypts in contrast to the data discussed above for the small intestine. Preliminary simulations of the colon crypt using the model concept presented here suggest that the colonic crypts are characterized by much steeper relationships in the S_f-r diagrams shown in Fig. 5 indicating that the fission threshold for colonic crypts is as low as 4 provided r is sufficiently large ($r > 0{\cdot}9$).

There are some limitations to the model presented here. First, the assumption may be challenged that crypt size is proportional to the number of stem cells (assumption 4). This would imply that differentiating cells originating from stem cells undergo a fixed number of cell divisions before final maturation. Experimental data supporting the idea of such a genetically fixed intrinsic pedigree program was recently reported by Rubin *et al.* (1991). In elegant studies using transgenic mouse intestinal isografts it could be shown that the differentiation program and the spatial arrangement of cells in subcutaneously grown isografts mimicked the pattern in normal intestinal crypts. However, further evidence for the pedigree concept of differentiating cells is still warranted. Second, it should be noticed that no mention was made to mutations in cells other than stem cells. There is now evidence that proliferating transit cells, and possibly also mature villus cells, can mutate following MNNG treatment (Potten & Li, unpublished data). However, within a short time of a few days these cells would have migrated onto the villus and will be shed. Thus, after only a few days to allow for this clearing, the mutations that are observed must originate from cells at the bottom of the crypt in the stem cell zone. Hence, the model presented here is not applicable to observations made in the first few days after application of a mutagen. Third, and more important, this model is only valid for the stationary state. This justifies the assumptions of constant values of the parameters t_c, p, q, and r. However, after damage to the crypt by irradiation or by cytotoxic drugs there is evidence that the parameters change (shorter t_c, increase in p, reduction in r) to support regeneration. These changes are likely to be the result of some regulation process which obviously renders the assumption of the independent single stem cell behaviour doubtful under such circumstances (see Potten & Loeffler, 1990). Future modelling will have to investigate how the above limiting assumptions can be relaxed and how stationary behaviour with stochastic elements and regulated behaviour with some state dependence of the parameters t_c, p, q, and r can be reconciled within one framework.

In summary, this paper showed that the phenomena associated with stem cell mutation and crypt conversion to monoclonality on one side and the phenomena of crypt fission and crypt size distribution on the other can be explained by the same theory. On the basis of present experimental knowledge the sets of parameters required to describe both phenomena overlap. More detailed experiments have been

proposed to establish this link more thoroughly and to identify the limitations of this approach.

This work has been supported by research grants of the Deutsche Forschungsgemeinschaft (Lo 342/4-1) and the Cancer Research Campaign and by a travel grant of the DAAD (FRG) and the British Council (UK). We thank Dr B. Grossmann (Heidelberg), Dr Peter Bauer (Koeln) and Dr Ursula Paulus (Koeln) for helpful discussions.

REFERENCES

CAIRNS, J. (1975). Mutation, selection and the natural history of cancer. *Nature, Lond.* **255,** 197–200.

GRIFFITHS, D. F. R., DAVIES, S. J., WILLIAMS, D., WILLIAMS, G. T. & WILLIAMS, E. D. (1988). Demonstration of somatic mutation and colonic crypt clonality by X-linked enzyme histochemistry. *Nature, Lond.* **333,** 461–463.

LOEFFLER, M. & GROSSMANN, B. (1991). A stochastic branching model with formation of subunits applied to the growth of intestinal crypts. *J. theor. Biol.* **150,** 175–191.

LOEFFLER, M., STEIN, R., WICHMANN, H. E., POTTEN, C. S., KAUR, P. & CHWALINSKI, S. (1986). Intestinal cell proliferation. I. A comprehensive model of steady-state proliferation in the crypt. *Cell Tissue Kinet.* **19,** 627–645.

MEINZER, H. P., SANDBLAD, B. & BAUR, H. J. (1992). Generation-dependent control mechanisms in cell proliferation and differentation. The power of two. *Cell Prolif.* **25,** 125–140.

POTTEN, C. S. (1990). A comprehensive study of the radiobiological response of the murine (BDF1) small intestine. *Int. J. Radiat. Biol.* **58,** 925–973.

POTTEN, C. S. & LOEFFLER, M. (1987). A comprehensive model of the crypts of the small intestine of the mouse provides insight into the mechanisms of cell migration and the proliferation hierarchy. *J. theor. Biol.* **127,** 381–391.

RUBIN, D. C., ROTH, K. A., BIRKENMEIER, E. H. & GORDON, J. I. (1991). Epithelial cell differentiation in normal and transgenic mouse intestinal isograft. *J. Cell Biol.* **113,** 1183–1192.

POTTEN, C. S. & LOEFFLER, M. (1990). Stem cells: attributes, cycles, spirals, pitfalls and uncertainties. Lesson for and from the crypt. *Development* **110,** 1001–1018.

WINTON, D. J., BLOUNT, M. A. & PONDER, B. A. (1988). A clonal marker induced by mutation in mouse intestinal epithelium. *Nature, Lond.* **333,** 463–466.

WINTON, D. J. & PONDER, B. A. (1990). Stem cell organization in mouse small intestine. *Proc. R. Soc. Lond. B* **241,** 13–18.

APPENDIX

Mathematical Methodology

In order to solve the above problems the model approach originally used by Loeffler & Grossmann (1991) had to be modified. They were not interested in pursuing the fate of individual crypts, but rather in obtaining the asymptotically stable distribution of stem cells per crypt averaged over a large population. However, in order to describe the conversion of crypts due to single cell mutations, explicit consideration of single cells was inevitable. To achieve this aim Monte Carlo calculations were performed. The following procedure was chosen:

TYPES OF CRYPTS

Let t be an integer variable counting time steps. Let P^*, N^*, M^*, A^* denote the sets of P-monoclonal, N-monoclonal and mixed crypts and all crypts at a given moment t. A crypt $h \in A^*$ consists of a number of P-stem cells and N-stem cells. Let

$S_h(t)$ denote the size of crypt h at time t, let $P_h(t)$ and $N_h(t)$ denote the number of positive and negative stem cells in the crypt h ($S_h = N_h + P_h$), then one can write

$$P^* = \{h \in A^* \mid P_h(t) > 0,\ N_h(t) = 0\}$$
$$N^* = \{h \in A^* \mid P_h(t) = 0,\ N_h(t) > 0\}$$
$$M^* = \{h \in A^* \mid P_h(t) > 0,\ N_h(t) > 0\}$$
$$A^* = P^* \cup N^* \cup M^*.$$

Let P, N, M and C denote the size of each of these sets ($A = P + N + M$). Likewise one can subdivide the mixed crypts into four disjunct classes

$$M_{\mathrm{I}}^* = \{h \in M^* \mid 0 < N_h(t)/(N_h(t) + P_h(t)) < 0{\cdot}25\}$$
$$M_{\mathrm{II}}^* = \{h \in M^* \mid 0{\cdot}25 \leq N_h(t)/(N_h(t) + P_h(t)) < 0{\cdot}5\}$$
$$M_{\mathrm{III}}^* = \{h \in M^* \mid 0{\cdot}5 \leq N_h(t)/(N_h(t) + P_h(t)) < 0{\cdot}75\}$$
$$M_{\mathrm{IV}}^* = \{h \in M^* \mid 0{\cdot}75 \leq N_h(t)/(N_h(t) + P_h(t)) < 1{\cdot}0\}$$

with M_{I}, M_{II}, M_{III} and M_{IV} denoting the sizes of the respective sets ($M = M_{\mathrm{I}} + M_{\mathrm{II}} + M_{\mathrm{III}} + M_{\mathrm{IV}}$). Furthermore it is helpful to introduce a set denoting the detectable mixed crypts

$$M_d^* = \{h \in M^* \mid d \leq N_{h(t)}/(N_h(t) + P_h(t)) < 1\} \text{ and } 1 > d \geq 0.$$

Note that each of these sets is time dependent and, by definition, crypts which have no cells any more [i.e. $N_h(t) = P_h(t) = 0$] are removed at each time step (extinction). At any time point one can evaluate the number of N-monoclonal, P-monoclonal and mixed crypts as $N(t)$, $P(t)$ and $M(t)$.

GROWTH PROCESS

The time development of individual crypts depends on the cellular growth process and on the crypt fission process in the following way:

(a) Stem cell growth: For each crypt $h \in A^*$ containing $S_h(t)$ stem cells at time t, S_h random numbers are generated in order to decide for each cell with probabilities p, r and q whether it produces two, one or zero offspring stem cells, respectively. Each of the offspring maintains the P or N marker of its mother cell. This generates $N_h(t+1)$ and $P_h(t+1)$ negative and positive stem cells in crypt h.

(b) Crypt fission: If $S_h(t+1) = N_h(t+1) + P_h(t+1) > S_f$ holds the crypt fission process is considered. Assuming binominal statistics each of the $S_h(t+1)$ cells is allocated to one of two daughter crypts with probability 1/2 again maintaining its marker.

Consequently one obtains the transition probability P_{ij} for a crypt of size $S(t) = i$ in generation t to one of size $S(t+1) = j$ in generation $t+1$ as given by eqns (2a–e) in Loeffler & Grossmann (1991).

EVALUATIONS

(a) Frequencies of monoclonal and mixed crypts: With the above definitions one can calculate useful quantities, for example:

$A(t)=N(t)+P(t)+M(t)$: total number of crypts

$N(t)/A(t)$; $M(t)/A(t)$; $M_d(t)/A(t)$; $P(t)/A(t)$: fraction of N-monoclonal, mixed, detectable mixed or P-monoclonal crypts of all crypts. This is used in Fig. 4(a) and (c).

$N(t)/(N(t)+M_d(t))$: fraction of N-monoclonal crypts of all crypts containing detectable N-cells. This is used in Fig. 4(b).

$N_\infty=\lim_{t\to\infty} N(t)/A(t)$: asymptotic fraction of N-monoclonal crypts established.

(b) Frequency distribution of stem cells per crypt: At any given time t one can evaluate the frequency distribution of stem cells per crypt. Let A^*_m denote the set of crypts which have m stem cells ($m>0$)

$$A^*_{m,}=\{h\in A^* \mid S_h(t)=m,\ m>0\}$$

and $A_m(t)$ its respective size. One can then define the relative frequency of stem cells per crypt: $f_m(t)=A_m(t)/A(t)$. This is used in Fig. 3.

(c) Time of monoclonality conversion: An important evaluation concerns the time it takes to convert to monoclonality. Experimentally one can evaluate the time course of the ratio $N(t)/[N(t)+M_d(t)]$. As mixed crypts disappear in the long run this quantity finally approaches 1. It is convenient to evaluate the time t^* at which a 90%-conversion to N-monoclonality is obtained [i.e. for which $N(t^*)/[N(t^*)+M_d(t^*)]=0{\cdot}9$].

(d) Crypt life time: Owing to extinction and fission, crypts have only a limited lifetime. It is possible to record all life times in a model simulation and to obtain a lifetime distribution. Clearly the life time of crypts is different from the average doubling time T of the crypt population.

NUMERICAL REALIZATION

Initial condition

Simulations usually started with several thousand crypts with a random number of stem cells ($<S_f$) in each. The simulations were performed until a stationary distribution of stem cells per crypt was obtained. The criterion of stationarity adopted was that the L_2 measure of two distributions obtained in successive iteration steps should be smaller than 10^{-4}. Usually this occurred within 1000 generation steps.

Initial sample of crypts containing one mutated cell

As soon as the stationary state was achieved a population of crypts was sampled in which exactly one cell is converted to N-state. This was achieved by generating a stratified random sample of crypts giving crypts with K-stem cells the weight K/S_f to be drawn from the stationary distribution ($K=1,\ldots,S_f$). This accounts for the

fact that crypts with more stem cells have a proportionally higher chance to contain a mutated stem cell. Thus this procedure was consistent with assumption 5A. The subsequent simulations were performed for 300 generations with evaluations at five generation intervals.